

Open charm measurements in NA61/SHINE at CERN SPS

Pawel Staszal for the NA61/SHINE Collaboration
Jagiellonian University Institute of Physics,
ul. Lojasiewicza 11, 30-348 Krakow, PL

November 25, 2021

Abstract

The measurements of open charm production was proposed as an important tool to investigate the properties of hot and dense matter formed in nucleus-nucleus collisions as well as to provide the means for model independent interpretation of the existing data on J/ψ suppression. Recently, the experimental setup of the NA61/SHINE experiment was supplemented with a Vertex Detector which was motivated by the importance and the possibility of the first direct measurements of open charm meson production in heavy ion collisions at SPS energies. First test data taken in December 2016 on Pb+Pb collisions at $150A$ GeV/ c allowed to validate the general concept of D^0 meson detection via its $D^0 \rightarrow \pi^+ + K^-$ decay channel and delivered a first indication of open charm production.

The physics motivation of open charm measurements at SPS energies, pilot results on open charm production, and finally, the future plans of open charm measurements in the NA61/SHINE experiment after LS2 are presented.

1 Introduction

The SPS Heavy Ion and Neutrino Experiment (NA61/SHINE) [1] is a fixed-target experiment located at the CERN Super Proton Synchrotron (SPS). The NA61/SHINE detector is optimized to study hadron production in hadron-proton, hadron-nucleus and nucleus-nucleus collisions. The strong interaction research program of NA61/SHINE is dedicated to the study of the properties of the onset of deconfinement and the search for the critical point of strongly interacting matter. These goals are being pursued by investigating p+p, p+A and A+A collisions at different beam momenta from $13A$ to $150A$ GeV/ c . In 2016 NA61/SHINE was upgraded with the Small Acceptance Vertex Detector (SAVD) based on MIMOSA-26AHR sensors developed in IPHC Strasbourg. Construction of this device was mostly motivated by the importance and the possibility of the first direct measurements of open charm meson production in

heavy ion collisions at SPS energies. Precise measurements of charm hadron production by NA61/SHINE are expected to be performed in 2022–2024. The related preparations have started already.

2 Physics motivation for open charm measurements

One of the important aspects of relativistic heavy-ion collisions is the mechanism of charm production. Several models were developed to describe charm production. Some of them are based on dynamical and others on statistical approaches. The estimates from these models for the average number of produced c and \bar{c} pairs ($\langle c\bar{c} \rangle$) in central Pb+Pb collisions at $158A$ GeV/c differ by up to a factor of 50 [2, 3] as illustrated in Fig. 1 (*left*). Therefore, obtaining precise

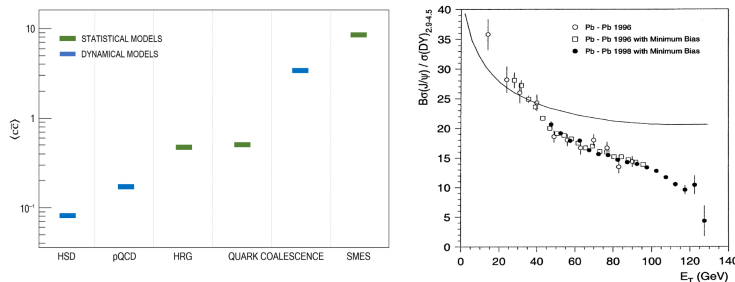


Figure 1: (*Left:*) Mean multiplicity of charm quark pairs produced in the full phase space in central Pb+Pb collisions at $158A$ GeV/c calculated with dynamical models (blue bars): HSD [4, 5], pQCD–inspired [6, 7], and Dynamical Quark Coalescence [8], as well as statistical models (green bars): HRG [9], Statistical Quark Coalescence [9], and SMES [10]. (*Right:*) The ratio of $\sigma_{J/\psi}/\sigma_{\text{DY}}$ as a function of transverse energy (a measure of collision violence or centrality) in Pb+Pb collisions at $158A$ GeV measured by NA50. The curve represents the J/ψ suppression due to ordinary nuclear absorption [11].

data on $\langle c\bar{c} \rangle$ will allow to distinguish between theoretical predictions and learn about the charm quark and hadron production mechanism. A good estimate of $\langle c\bar{c} \rangle$ can be obtained by measuring the yields of D^0 , D^+ and their antiparticles because these mesons carry about 85% of the total produced charm [12].

Charm mesons are of special interest in the context of the phase transition between confined hadronic matter and the quark gluon plasma (QGP). The $c\bar{c}$ pairs produced in the collisions are converted into open charm mesons and charmonia (J/ψ mesons and the excited states). The production of charm is expected to be different in confined and deconfined matter. This is caused by different properties of charm carriers in these phases. In confined matter the lightest charm carriers are D mesons, whereas in deconfined matter the lightest carriers are charm quarks. Production of a DD pair ($2m_D = 3.7$ GeV) requires

an energy about 1 GeV higher than production of a $c\bar{c}$ pair ($2m_c = 2.6$ GeV). The effective number of degrees of freedom of charm hadrons and charm quarks is similar [13]. Thus, in the statistical approach more abundant charm production is expected in deconfined than in confined matter. Consequently, in analogy to strangeness production [3, 14], a change of collision energy dependence of $\langle c\bar{c} \rangle$ may be a signal of the onset of deconfinement.

Figure 1 (*right*) shows results on $\langle J/\psi \rangle$ production normalized to the mean multiplicity of Drell-Yan pairs in Pb+Pb collisions at the top SPS energy obtained by the NA50 collaboration. The solid line shows a model prediction for normal nuclear absorption of J/ψ in the medium. NA50 observed that J/ψ production is consistent with normal nuclear matter absorption for peripheral collisions and is suppressed for more central collisions. This so called anomalous suppression was attributed to the J/ψ dissociation effect in the deconfined medium. However, the above result is based on the assumption that $\langle c\bar{c} \rangle \sim \langle DY \rangle$ which may be incorrect due to several effects, such as shadowing or parton energy loss [15]. Thus the effect of the medium on $c\bar{c}$ binding can only be quantitatively determined by comparing the ratio of $\langle J/\psi \rangle$ to $\langle c\bar{c} \rangle$ in nucleus-nucleus to that in proton-proton reactions. In Pb+Pb collisions the onset of color screening should already be seen in the centrality dependence of the $\langle J/\psi \rangle$ to $\langle c\bar{c} \rangle$ ratio. This clearly shows the need for large statistic data on $\langle c\bar{c} \rangle$.

3 Performance of SAVD

The SAVD was built using sixteen CMOS MIMOSA-26 sensors [16]. The basic sensor properties are: $18.4 \times 18.4 \mu\text{m}^2$ pixels, 115 μs time resolution, $10 \times 20 \text{ mm}^2$ surface, 0.66 MPixel, 50 μm thick. The estimated material budget per layer, including the mechanical support, is 0.3% of a radiation length. The sensors were glued to eight ALICE ITS ladders [17], which were mounted on two horizontally movable arms and spaced by 5 cm along the z (beam) direction. The detector box was filled with He (to reduce beam-gas interactions) and contained an integrated target holder to avoid unwanted material and multiple Coulomb scattering between target and detector. More details related to the SAVD project can be found in [18].

The first test of the device was performed in December 2016 during a Pb+Pb test run. The test allowed to demonstrate: tracking in a large track multiplicity environment, precise primary vertex reconstruction, TPC and SAVD track matching. Furthermore, it allowed to make a first search for the D^0 and \bar{D}^0 signals. The obtained primary vertex resolution along the beam direction of 30 μm was sufficient to perform the search for the D^0 and \bar{D}^0 signals. Figure 2 (*right*) shows the first indication of a D^0 and \bar{D}^0 peak obtained using the data collected during the Pb+Pb run in 2016.

Successful performance of the SAVD in 2016 led to the decision to also use it during the Xe+La data taking in 2017. About $5 \cdot 10^6$ events of central Xe+La collisions at 150A GeV/c were collected in October and November 2017. During

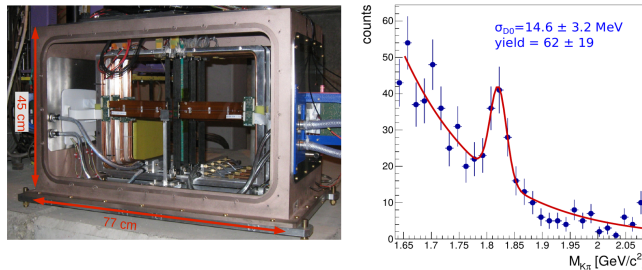


Figure 2: *Left:* The SAVD used by NA61/SHINE during the data taking in 2016 and 2017. *Right:* The invariant mass distribution of D^0 and \overline{D}^0 candidates in central Pb+Pb collisions at $150A$ GeV/ c after the background suppression cuts. The particle identification capability of NA61/SHINE was not used at this stage of the analysis [2].

these measurements the thresholds of the MIMOSA-26 sensors were tuned to obtain high hit detection efficiency which led to significant improvement in the primary vertex reconstruction precision, namely the spatial resolution of the primary vertices obtained for Xe+La data is on the level of $1 \mu\text{m}$ and $15 \mu\text{m}$ in the transverse and longitudinal coordinates, respectively. The distribution of the longitudinal coordinate (z_{prim}) of the primary vertex is shown in Fig. 3 (*left*) (see Ref. [2] for details) The Xe+La data are currently under analysis and are expected to lead to physics results in the coming months.

The SAVD will also be used during three weeks of Pb+Pb data taking in 2018. About $1 \cdot 10^7$ central collisions should be recorded and 2500 D^0 and \overline{D}^0 decays can be expected to be reconstructed in this data set.

4 Proposed measurements after LS2

During the Long Shutdown 2 at CERN (2019-2020), a significant modification of the NA61/SHINE spectrometer is planned. The upgrade is primarily motivated by the charm program which requires a tenfold increase of the data taking rate to about 1 kHz and an increase of the phase-space coverage of the Vertex Detector by a factor of about 2. This, in particular, requires construction of a new Vertex Detector (VD), replacement of the TPC read-out electronics, implementation of new trigger and data acquisition systems and upgrade of the Projectile Spectator Detector. Finally, new ToF detectors are planned to be constructed for particle identification at mid-rapidity. This is mainly motivated by possible future measurements related to the onset of fireball formation. The detector upgrades are discussed in detail in Ref. [2]. The data taking plan related to the open charm measurements foresees measurements of 500M inelastic Pb+Pb collisions at $150A$ GeV/ c in 2022 and 2023. This data will provide the mean number of $c\bar{c}$ pairs in central Pb+Pb collisions needed to investigate the mechanism of charm production in this reaction. Moreover, the data will allow to establish

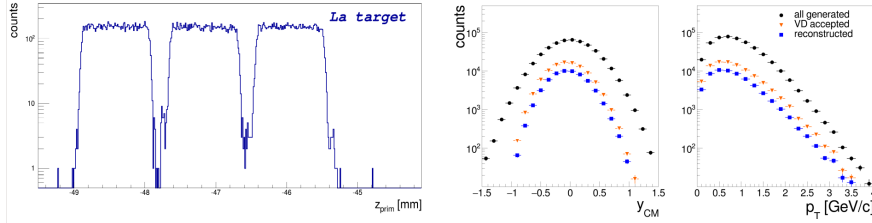


Figure 3: (*Left:*) Distribution of longitudinal coordinate of the primary vertex z_{prim} for interactions in the La target, which was composed of three 1 mm plates. *Right:* Rapidity (*left*) and transverse momentum (*right*) distributions of $D^0 + \bar{D}^0$ mesons produced in about 500M inelastic Pb+Pb collisions at 150A GeV/c. Dots indicate all generated mesons, triangles mesons within the VD acceptance and squares mesons within the VD acceptance and passing background suppression cuts.

the centrality dependence of $\langle c\bar{c} \rangle$ in Pb+Pb collisions at 150A GeV/c and thus address the question of how the formation of QGP impacts J/ψ production. Table 1 lists the expected number of charm mesons in centrality selected Pb+Pb collisions at 150A GeV/c assuming the above mentioned statistics of minimum bias collisions. The estimate was performed assuming that the mean multiplicity of charm hadrons is proportional to the number of collisions and used yields calculated for central Pb+Pb collisions within the HSD model [4, 5]. Central (0-30%) Pb+Pb collisions at 40A GeV/c are planned to be recorded in 2024. This data together with the result for central Pb+Pb collisions at 150A GeV/c will start a long-term effort to establish the collision energy dependence of $\langle c\bar{c} \rangle$ and address the question of how the onset of deconfinement impacts charm production. The expected high statistics of reconstructed D^0 and \bar{D}^0 decays is due to

Table 1: Expected number of charm mesons in centrality selected Pb+Pb collisions at 150A GeV/c assuming 500M minimum bias events recorded in 2022 and 2023, see text for detail. The mean number of wounded nucleons $\langle W \rangle$ calculated within the Wounded Nucleon Model is also given.

	0-10%	10-20%	20-30%	30-60%	60-90%	0-90%
$\#(D^0 + \bar{D}^0)$	31k	20k	11k	13k	1.3k	76k
$\#(D^+ + D^-)$	19k	12k	7k	8k	0.8k	46k
$\langle W \rangle$	327	226	156	70	11	105

the high event rate and the relatively large efficiencies of open charm detection in the VD. The efficiency will be about 13% (3 times better than for the SAVD) for the $D^0 \rightarrow \pi^+ + K^-$ decay channel and about 9%¹ for D^+ decaying into $\pi^+ + \pi^+ + K^-$.

¹The quoted efficiencies include the geometrical acceptance for $D^0 \rightarrow \pi^+ + K^-$ ($D^+ \rightarrow \pi^+ + \pi^+ + K^-$) decays and the efficiency of the analysis quality cuts used to reduce the combinatorial background.

Figure 3 (*right*) shows distributions of $D^0 + \overline{D}^0$ mesons in rapidity and transverse momentum for all generated particles (black symbols) and for particles that passed the acceptance and background reduction cuts (blue symbols). The presented plots refer to 500M inelastic Pb+Pb collisions at 150A GeV/c. Total uncertainty of $\langle D^0 \rangle$ and $\langle \overline{D}^0 \rangle$ is expected to be about 10% and is dominated by systematic uncertainty.

In summary it is emphasized that only NA61/SHINE is able to measure open charm production in heavy ion collisions in full phase space and at the beginning of the next decade. The corresponding potential measurements at higher (LHC, RHIC) and lower (FAIR, J-PARC) energies are necessary to complement the NA61/SHINE results and establish the collision energy dependence of charm production.

Acknowledgments: this work was supported by the Polish National Center for Science grants 2014/15/B/ST2/02537 and 2015/18/M/ST2/00125.

References

- [1] N. Abgrall *et al.*, [NA61/SHINE Collab.] JINST 9 (2014) P06005.
- [2] A. Aduszkiewicz *et al.*, [NA61/SHINE Collaboration], CERN-SPSC-2017-038/CERN-SPSC-2018-008/SPSC-P-330-ADD-10.
- [3] M. Gazdzicki, M.I. Gorenstein, 1999, Acta Phys. Pol. B 30, 2705.
- [4] O. Linnyk, E. L. Bratkovskaya and W. Cassing, Int. J. Mod. Phys. E17 (2008) 1367.
- [5] T. Song, private communication.
- [6] R. Gavai, *et al.*, Int. J. Mod. Phys. A10 (1995) 2999.
- [7] P. Braun-Munzinger, and J. Stachel, Phys. Lett. B490 (2000) 196
- [8] P. Levai, *et al.*, J. Phys. G27 (2001) 703.
- [9] A. P. Kostyuk *et al.*, Phys. Lett. B531 (2002) 195.
- [10] M. Gazdzicki and M.I. Gorenstein, Acta Phys. Pol. B30 (1999) 2705.
- [11] M. C. Abreu, *et al.*, Phys. Lett. B477 (2000) 28.
- [12] W. Cassing, E.L. Bratkovskaya, Nucl.Phys. A831 (2009) 215.
- [13] R. V. Poberezhnyuk, M. Gazdzicki, and M. I. Gorenstein, Acta Phys. Pol. B 48, (2017) 146.1
- [14] J. Rafelski and B. Muller, Phys. Rev. Lett. 48, (1982) 1066.

- [15] H. Satz, EPJ Web Conf. 71. (2014) 00118., H. Satz *Adv. High Energy Phys.* **2013**, (2013) 242918.
- [16] MIMOSA26 User Manual: www.iphc.cnrs.fr/IMG/pdf/M26_UserManual_light.pdf
- [17] B. Abelev, *et al.*, [ALICE Collaboration], 2013, CERN-LHCC-2013-024 / ALICE-TDR-017.
- [18] M. Deveaux *et al.*, EPJ Web of Conf. 171, 10003 (2018).